The Generation of Correlated Rayleigh Random Variates by Inverse Discrete Fourier Transform

David J. Young, *Student Member, IEEE*, and Norman C. Beaulieu, *Fellow, IEEE*

***Abstract*—A number of different algorithms are used for the generation of correlated Rayleigh random variates. This paper presents an analysis of the statistical properties of methods based on the inverse discrete Fourier transform (IDFT). A modification of the algorithm of Smith is presented, the new method requiring exactly one-half the number of IDFT operations and roughly two-thirds the computer memory of the original method. Evaluations of and comparisons between various variate generation methods using meaningful quantitative measures are believed to be lacking. Recently, new quantitative quality measures for random variate generation have been proposed that are, in particular, meaningful and useful for digital communication system simulation. This paper presents the application of these measures to the IDFT method and three other methods of correlated variate generation, comparing the algorithms in terms of the quality of the generated samples and the required computational effort.**

***Index Terms*—Multipath channels, random number generation, simulation.**

I. Introduction

DIGITAL computer simulation is widely used in the design and performance assessment of communications components and systems. Many simulation packages and designs for land mobile and macrocellular systems require the input of random variates having a Rayleigh distribution. It is well known that discrete-time samples of a realistic Rayleigh fading process must necessarily be correlated, and that the correlation function is dependent on the Doppler frequency corresponding to the relative motion of the receiver and transmitter as well as other factors, such as antennae characteristics and propagation path. A number of different algorithms have been proposed and used for the generation of correlated Rayleigh random variates [1]–[5]. Evaluations of and comparisons between various variate generation methods using meaningful quantitative measures are believed to be lacking, however. This paper first addresses the problem of generation of correlated Rayleigh random variates, providing useful analysis and modification to a popular algorithm based on the inverse discrete Fourier transform (IDFT). The paper also provides a quantitative evaluation of four methods of random variate generation, comparing the algorithms in terms of the quality of the generated samples and the required computational effort. Despite the need for efficient and statistically accurate generation of such variates, it is believed that a similar quantitative comparison is lacking in the published literature, and hence these results have importance for designers of mobile communication systems.

The IDFT algorithm for generation of correlated Rayleigh random variates was presented by Smith as FORTRAN code in [1] and has been widely utilized in simulations of wireless systems [6], [7]. In the method, the IDFT operation is applied to complex sequences of independent, normally distributed random numbers, each sequence weighted by appropriate filter coefficients. An analysis of the algorithm output, needed to understand and justify the statistical properties of IDFT methods, is absent in [1] and provided by this paper. More importantly, this paper provides a new and powerful modification to the algorithm. The new method is superior to that of [1] in that it requires exactly one-half the number of IDFT operations and roughly two-thirds of the computer memory required by the latter, while yielding variates with identical statistical properties. In addition, we also present a simple modification to either algorithm that can be used to generate Ricean random variates.

Evaluations of and comparisons between random variate generation methods often are provided using qualitative methods. For example, [3] and [8]–[10] appeal to qualitative visual inspection of random sample autocorrelation functions, [3], [5], and [11] include plots of first-order empirical cumulative distribution functions or first-order empirical probability density functions (pdf's), and [1] and [5] plot actual generator output for direct inspection. Plots of level crossing rates and average fade durations are also used [9], [11]. Such qualitative techniques, in addition to being imprecise, often yield information that does not necessarily have a direct relationship to the quality of the variates.

Quantitative techniques have been used in the published literature, but these also often do not have a clear relationship to the quality of variates for simulation applications. For example, the mean-square error of the autocorrelation function over a specified interval is used for algorithm design and comparison in [5]. Also, a weighted mean-square autocorrelation error is used to evaluate generator performance in [12]. Justification for the use of these measures is not provided, however, and the relationship of either measure to simulation quality is not evident. Moreover, such tests ignore important differences between autocorrelation functions evident even in qualitative comparison.

Quantitative quality measures of random variate generation have been proposed [13]–[15] that are, in particular, meaningful

Paper approved by Z. Kostic, the Editor for Wireless Communication of the IEEE Communications Society. Manuscript received July 12, 1998; revised November 3, 1998 and October 20, 1999. This paper was presented in part at the 1996 IEEE International Conference on Universal Personal Communications (ICUPC'96), Cambridge, MA, September 1996, and in part at the 1998 Global Telecommunications Conference (GLOBECOM'98), Sydney, Australia, November 1998.

The authors are with the Department of Electrical and Computer Engineering, Queen's University, Kingston, ON K7L 3N6, Canada (e-mail: beaulieu@ee.queensu.ca).

Publisher Item Identifier S 0090-6778(00)06153-5.

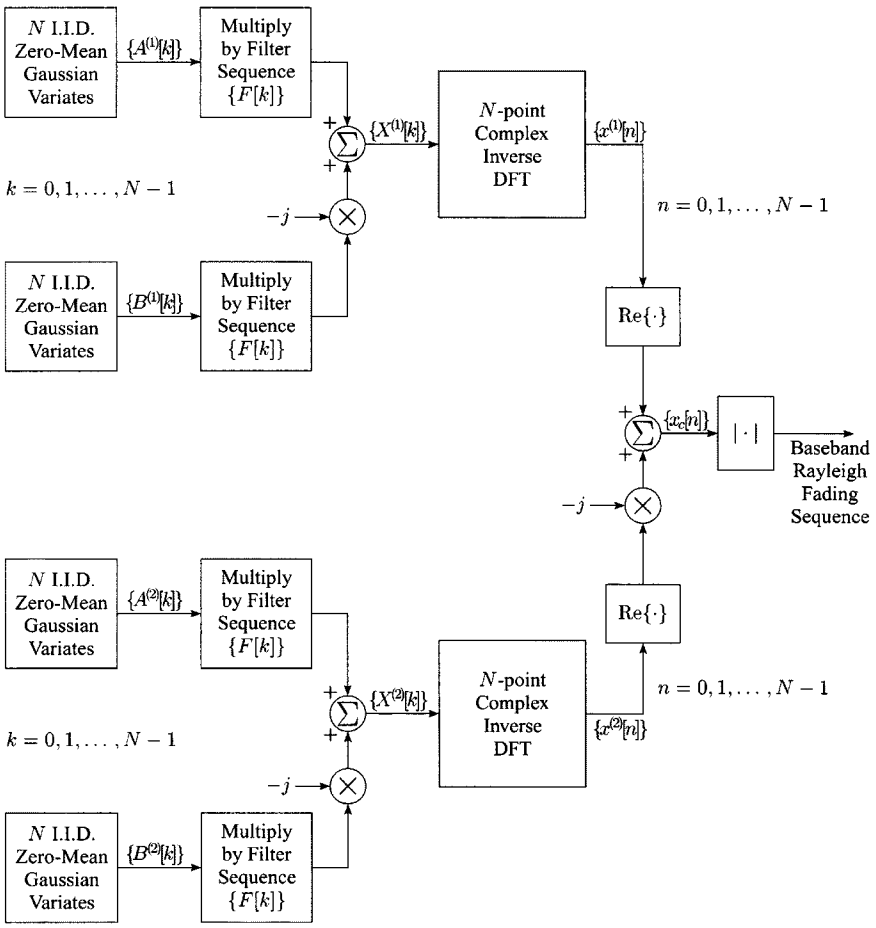

Fig. 1. Block diagram of the algorithm of Smith to generate correlated Rayleigh variates.

and useful for digital communication system simulation. These new quality measures are used in this paper to assess comparatively four important methods of generating correlated Rayleigh variates. Specifically, the IDFT method, filtering of white Gaussian noise (WGN) using the filter design of [14] and [16], filtering of WGN using a third-order Butterworth filter, and the Monte Carlo superposition of sinusoids method [4] are evaluated in terms of the quality of the generated samples and the required computational effort.

This paper has the following structure. Section II presents a description and analysis of the IDFT method. Section III gives the modification to the algorithm reducing the required computational resources. Section IV presents a detailed explanation of specific filter coefficients used in the routine of [1] to model the received signal at a vertical monopole antenna under isotropic scattering, and investigates the possibility of improving this filter. Section V presents the quantitative comparison of random variate generation algorithms. A brief overview of the measures and the methods to be compared is provided in that section, as well as the results of evaluations based on sample quality and computational effort. Finally, some conclusions are given in Section VI.

II. Statistical Properties of IDFT Method

In Sections II and III, we present the algorithms without defining filter coefficients as the methods are applicable to a wide variety of autocorrelation function specifications. A specific filter useful for simulation of many mobile communication channels will be defined in Section IV.

A. Description and Analysis of IDFT Output

The desired algorithm output is a Rayleigh-distributed sequence with specified correlation properties. This Rayleigh-distributed output sequence is formed by taking the magnitude of a zero-mean complex Gaussian sequence, the real and imaginary parts of which are independent and identically distributed (i.i.d.) [17, p. 140]. In Fig. 1, we present a block diagram of the Smith algorithm. Generation of the in-phase component of the fading process is represented by the upper half of the diagram; generation of the quadrature component is identical and represented by the lower half. In each case, the algorithm starts with two independent sequences of i.i.d. random variates, here denoted $\{A[k]\}$ and $\{B[k]\}$, $k = 0, 1, \cdots, N-1$. Each variate has a normal distribution with zero mean and variance σ^2; that is

$$E\{A[k]\} = E\{B[k]\} = 0 \tag{1}$$

and

$$E\left\{A^2[k]\right\} = E\left\{B^2[k]\right\} = \sigma^2. \tag{2}$$

The independence between variates implies

$$E\{A[k]A[l]\} = E\{B[k]B[l]\} = 0, \qquad k \neq l \tag{3}$$

and

$$E\{A[k]B[l]\} = 0 \qquad \forall k, l. \tag{4}$$

Several well-tested routines to generate such variates are found in the literature [18]–[20].

The sequences are each weighted by a sequence of filter coefficients $\{F[k]\}$, and added in quadrature to form the complex Gaussian sequence $\{X[k]\}$. An IDFT is then taken of this complex sequence to form complex time samples, which for the in-phase branch will here be denoted $\{x^{(1)}[n]\}$. We will see that the statistics of the real and imaginary parts of the complex sequence are identical, each approximating the real or imaginary part of the baseband fading signal. The two parts at the output of the IDFT in Smith's algorithm are correlated, however, and our tests have shown they cannot both be used to form the desired sequence of Rayleigh variates. Hence, the real part, $\mathrm{Re}\{x^{(1)}[n]\}$, is added in quadrature with the real part from a second identical and independent branch, $\mathrm{Re}\{x^{(2)}[n]\}$, producing complex samples which model the fading channel accurately. The imaginary parts of each sequence are discarded. In the original routine, the magnitude of the complex samples is taken, expressed in decibels in the output of the program. In computer implementation, the sequence $\mathrm{Re}\{x^{(1)}[n]\}$ is generated first, stored, and then the identical set of operations is repeated to generate $\mathrm{Re}\{x^{(2)}[n]\}$.

To justify the use of the IDFT algorithm, we must find the pdf of the sequences $\mathrm{Re}\{x^{(1)}[n]\}$ and $\mathrm{Re}\{x^{(2)}[n]\}$ and compare this to the correct pdf. It is necessary also to determine the autocorrelation function of each sequence. The sequences at the output of the in-phase and quadrature branch complex IDFT's, $\{x^{(1)}[n]\}$ and $\{x^{(2)}[n]\}$, respectively, are statistically identical, so we will use the notation $\{x[n]\}$ to represent either sequence since it is not necessary to distinguish the particular branch in question.

Considering the description of this sequence $\{x[n]\}$, therefore, we start by forming its discrete Fourier transform (DFT) sequence, denoted $\{X[k]\}$, $k = 0, 1, \cdots, N-1$, where

$$X[k] = F[k]A[k] - jF[k]B[k]. \tag{5}$$

The elements of sequence $\{F[k]\}$ are the real-valued filter coefficients, the values of which will be specified in Section IV. We note that restricting the filter to be real does not make the analysis less general. It can be shown that a complex filter is equivalent in the algorithm to a real filter with coefficients $\{F[k]\}$ given by the complex coefficient magnitudes.

Taking the IDFT, we have

$$x[n] = \frac{1}{N} \sum_{k=0}^{N-1} \left(F[k]A[k] - jF[k]B[k]\right) e^{j(2\pi kn/N)}. \tag{6}$$

The output of the IDFT can be expressed as $x[n] = x_R[n] + jx_I[n]$, where $x_R[n] = \mathrm{Re}\{x[n]\}$ and $x_I[n] = \mathrm{Im}\{x[n]\}$. We wish to determine the joint statistical properties of these two sequences. Each of $x_R[n]$ and $x_I[n]$ is composed of a weighted sum of $2N$ jointly Gaussian random variables, as can be observed in Appendix A, (A.1), and (A.2). Therefore, $x_R[n]$ and $x_I[n]$ also each have a joint Gaussian distribution. This is a consequence of the fact that a linear operation, such as the IDFT, performed on jointly Gaussian samples will yield samples that also have a joint Gaussian distribution. It is therefore sufficient to find the *means* of each sequence, $E\{x_R[n]\}$ and $E\{x_I[n]\}$, the *autocorrelations* of each sequence, $r_{RR}[m,n] = E\{x_R[m]x_R[n]\}$ and $r_{II}[m,n] = E\{x_I[m]x_I[n]\}$, and the *cross-correlation* between the sequences, $r_{RI}[m,n] = E\{x_R[m]x_I[n]\}$, to fully determine the joint distribution of $\{x_R[n]\}$ and $\{x_I[n]\}$. Derivation of each of these statistics is given in Appendix A. The means of each sequence are there shown to be zero. The autocorrelation sequences of both real and imaginary parts can be written as

$$r_{RR}[m,n] = r_{II}[m,n] = r_{RR}[d] = r_{II}[d] = \frac{\sigma^2}{N} \mathrm{Re}\{g[d]\} \tag{7}$$

and the cross-correlation sequence between the real part and the imaginary part is

$$r_{RI}[m,n] = r_{RI}[d] = \frac{\sigma^2}{N} \mathrm{Im}\{g[d]\} \tag{8}$$

where $d \equiv n - m$ is the *sample lag* and the sequence $\{g[d]\}$ is defined by

$$\{g[d]\} \overset{\mathrm{DFT}}{\longleftrightarrow} \left\{(F[k])^2\right\}. \tag{9}$$

The sequence $\{x[n]\}$ is stationary, since the autocorrelation depends only on the distance between the samples d, and ergodic, as shown in Appendix B. The autocorrelation of both the real and imaginary parts of the IDFT output depends on only the real part of $\{g[d]\}$, while the cross-correlation between the real and imaginary parts depends only on the imaginary part of $\{g[d]\}$. Two independent realizations of the process $\{x[n]\}$ are formed, earlier labeled $\{x^{(1)}[n]\}$ and $\{x^{(2)}[n]\}$, to guarantee that the quadrature sum will have a Rayleigh distribution. The real part of each is taken and the Rayleigh output sequence $\{|x_c[n]|\}$ is formed as

$$|x_c[n]| = \sqrt{\left(\mathrm{Re}\left\{x^{(1)}[n]\right\}\right)^2 + \left(\mathrm{Re}\left\{x^{(2)}[n]\right\}\right)^2}.$$

If $\{(F[k])^2\}$ is suitably chosen such that the real part of $\{g[d]\}$ approximates the desired autocorrelation, then the Smith algorithm will produce samples with good statistical properties.

B. Obtaining a Rayleigh Distribution or a Ricean Distribution

The desired output from the routine is a Rayleigh-distributed process. We note that a *given realization* of the IDFT output sequence will have mean given by a time average (see Appendix B), and for N finite and $F[0]$ nonzero, this time average is a zero-mean Gaussian random variable, taking on the exact value zero with probability zero. If the complex Gaussian process has nonzero mean, the output will have a Ricean distribution. That is, a given sample will have pdf [21]

$$p_R(r) = \frac{r}{\sigma^2} e^{-(r^2+s^2)/2\sigma^2} I_0\left(\frac{rs}{\sigma^2}\right), \qquad r \geq 0 \tag{10}$$

where $I_0(x)$ is the zeroth-order modified Bessel function of the first kind and the parameter s^2 is called the noncentrality parameter [21, p. 30]. When $s = 0$, (10) reduces to the Rayleigh

density function; however, it can be shown that for finite N and $F[0]$ nonzero, the expected value of s is a small but nonzero positive number. The only way to ensure that the expected value of s is zero is to require $F[0] = 0$. In this case, the variance of s is also zero—s is identically zero in every realization, a desirable property. Thus, for Rayleigh fading the requirement is made that the zero-frequency coefficient be set to zero, as in the program code of [1].

If, on the other hand, a Ricean process is desired, this can be achieved by setting the zero-frequency term $X[0]$ to a *deterministic* value according to the desired noncentrality parameter. It is straightforward to show that a Rice distribution with noncentrality parameter s is obtained when $X[0]$ satisfies the relation

$$|X[0]| = Ns. \tag{11}$$

To the best of the author's knowledge, this simple but useful modification to the algorithm has not been proposed previously.

III. Modification to the Existing Method

The sequence at the output of the algorithm as given in [1] does have statistical properties that closely match theory, but it is possible to generate statistically identical samples with only a single IDFT operation and consequently make better use of computer resources. We have stated the necessity of independence between the real and imaginary parts of the complex Gaussian sequence used to form the Rayleigh process. In the algorithm of [1] as presented in Section II, the complex output sequence from a single IDFT step does not have this property, so two such sequences must be formed independently, and the imaginary part of each sequence is discarded. It will now be shown that the output of a single IDFT can be used directly, by properly modifying the filter coefficients. Key to the modification is the fact that the autocorrelation sequences $\{r_{RR}[d]\}$ and $\{r_{II}[d]\}$ can be chosen independently from the cross-correlation sequence $\{r_{RI}[d]\}$.

A sequence $\{G_{\rm CS}[k]\}$ for which $G_{\rm CS}[k] = G^*_{\rm CS}[N-k]$ is known as a *conjugate-symmetric* sequence, while a sequence $\{G_{\rm CAS}[k]\}$ for which $G_{\rm CAS}[k] = -G^*_{\rm CAS}[N-k]$ is known as a *conjugate-antisymmetric* sequence [22], [23]. The IDFT of a conjugate-symmetric sequence has the property of being real. The IDFT of a conjugate-antisymmetric sequence is an imaginary sequence. Due to the linearity of the DFT operation, for a general sequence $\{g[d]\}$ with DFT $\{G[k]\}$

$$\begin{aligned} g[d] &= g_R[d] + jg_I[d] = \text{IDFT}\,\{G[k]\} \\ &= \text{IDFT}\,\{G_{\rm CS}[k]\} + \text{IDFT}\,\{G_{\rm CAS}[k]\} \end{aligned}$$

and

$$\begin{aligned} g_R[d] &= \text{Re}\,\{g[d]\} \overset{\text{DFT}}{\longleftrightarrow} \{G_{\rm CS}[k]\} \\ g_I[d] &= \text{Im}\,\{g[d]\} \overset{\text{DFT}}{\longleftrightarrow} \{G_{\rm CAS}[k]\}. \end{aligned} \tag{12}$$

We also note that

$$G_{\rm CS}[k] = \frac{1}{2}\,G[k] + \frac{1}{2}\,G^*[N-k] \tag{13}$$

and

$$G_{\rm CAS}[k] = \frac{1}{2}\,G[k] - \frac{1}{2}\,G^*[N-k]$$

for any sequence $\{G[k]\}$, where $G[k] = G_{\rm CS}[k] + G_{\rm CAS}[k]$, and the sequence $\{G[k]\}$ can always be expressed as the sum of conjugate-symmetric and conjugate-antisymmetric parts. We can therefore separately select the real and imaginary parts of the sequence $\{g[d]\}$, using, respectively, the two sequences $\{G_{\rm CS}[k]\}$ and $\{G_{\rm CAS}[k]\}$, and hence independently select the autocorrelation sequences and the cross-correlation sequence for the IDFT output $\{x[n]\}$.

To generate Rayleigh variates with a single IDFT, therefore, we require that $G_{\rm CAS}[k] = 0$ for all k, which will ensure zero cross-correlation between real and imaginary parts of the IDFT output. Using (13), we can thus define a modified filter $\{F_M[k]\}$, where

$$F_M[k] = \begin{cases} F_S[0], & k = 0 \\ \dfrac{1}{\sqrt{2}}\,F_S[k], & k = 1, 2, \cdots, \dfrac{N}{2} - 1 \\ F_S[k], & k = \dfrac{N}{2} \\ \dfrac{1}{\sqrt{2}}\,F_S[N-k], & k = \dfrac{N}{2} + 1, \cdots, N-1 \end{cases} \tag{14}$$

and $\{F_S[k]\}$ is a filter used in the Smith routine. Use of this modified filter in (6) will produce a complex Gaussian sequence with identical autocorrelation properties to Smith's original routine and the required independence between the real and imaginary parts.

Fig. 2 gives a block diagram of the new algorithm. This algorithm is simpler (compare Fig. 2 with Fig. 1), since the independence between the real and imaginary parts means that the complex output from a single IDFT is directly the complex Gaussian process we require to form the Rayleigh output sequence. The necessity of the second IDFT operation has been eliminated. This has two principal benefits.

First, the time to execute the procedure is reduced by almost one-half. The IDFT operations in the algorithm are implemented using an inverse fast Fourier transform (IFFT) routine [18]. The IFFT operations are the most computationally expensive part of the Smith procedure. Experimentation with the routines of [18] has shown that 85%–90% of the time to execute the routine is used in performing the IFFT operations. Halving the number of IFFT operations reduces the time to generate a given number of variates by 40%–45%. Fig. 3 shows this difference for routines coded in C and run on an UltraSPARC machine, using filters $\{F_S[k]\}$ and $\{F_M[k]\}$ band-limited to f_m, the maximum Doppler frequency normalized by the sample rate. The slight dependence of the run times on f_m occurs because in the case of a band-limited filter, some elements of the sequences $\{A[k]\}$ and $\{B[k]\}$ are multiplied by zero-valued filter coefficients, reducing the number of independent Gaussian variates required and saving a small amount of computation time.

Second, the memory use for the new routine is one-half to two-thirds that of the original. To perform the complex IFFT, $2N$ real storage locations are required. The real part from the

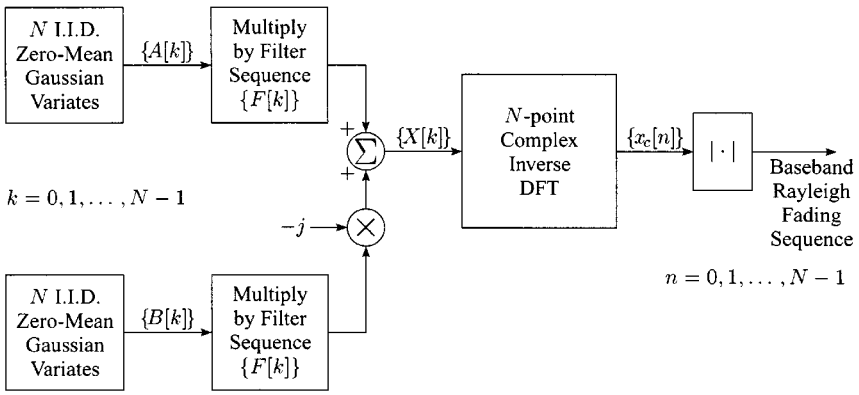

Fig. 2. Block diagram of the improved algorithm using a single complex IDFT to generate correlated Rayleigh variates.

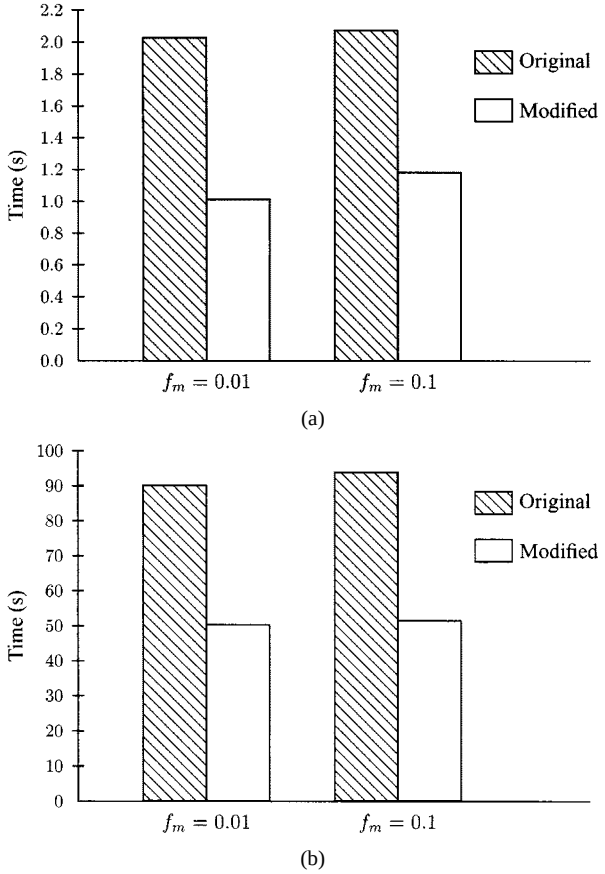

Fig. 3. Run times for the original and the modified IDFT algorithms. (a) 2^{16} samples. (b) 2^{21} samples.

first IFFT must be saved (using N storage locations), while the second IFFT is performed, for a total of $3N$ locations used. In some cases, however, such as the popular Numerical Recipes in C fast Fourier transform (FFT) routines [18], in which real and imaginary parts of a sequence alternate in a single real vector of length $2N$, or the IMSL FORTRAN FFT routines [24], which use a single complex array for input and output, storage for the real part from the first IFFT cannot be achieved without moving this data to new storage locations. In this situation, the most straightforward approach is to reserve $4N$ memory locations—one complex vector of length N for each IFFT operation is allocated and then the real part of each vector is added in quadrature at the conclusion of the routine. Thus, in order to generate N Rayleigh random variates, the original routine needs at least $3N$ storage locations for the data, and $4N$ locations are sometimes used. The modified routine requires $2N$ memory locations in either case, since only a single complex IFFT operation is required. Thus, we realize a savings of at least one-third, and possibly one-half, in computer memory usage. On a given machine, this means a larger sequence of correlated random variates can be generated without resorting to disk-based virtual memory (which lengthens execution time substantially).

As a further note, we mention that the desired variates can also be generated in an algorithm that uses two "real-sequence" IFFT's instead of the single complex IFFT. The real-sequence routine (as defined in, for example, [18, Sec. 12.3]) takes as input the first $N/2+1$ complex-valued DFT coefficients, and outputs the real length-N time sequence corresponding to a length-N symmetric DFT sequence. Relating the input filter of the real-sequence IFFT method, denoted $\{F_R[k]\}$, to $\{F_M[k]\}$, it can be shown [14] that

$$F_R[k] = F_M[k], \qquad k = 0, 1, \cdots, \frac{N}{2}. \tag{15}$$

The output from one real-sequence IFFT yields a real Gaussian sequence with the statistical properties of $\mathrm{Re}\{x[n]\}$. Two such sequences (from two independent runs) can be added in quadrature to form the desired Rayleigh variates. Use of the real-sequence IFFT does not offer significant advantages in the generation of Rayleigh variates, because two real sequences are required and this can be accomplished more easily with a single complex IFFT, routines for which are very common. However, the real-sequence IFFT method requires only N data points in memory at one time, an advantage when computer main memory is limited. Also, IDFT methods can be used to generate independent real Gaussian sequences with specified correlation properties (examined in [25]). The real-sequence IFFT approach is the only one of the IDFT methods that does not generate two real Gaussian sequences simultaneously, and thus is more efficient if only a single Gaussian sequence is required.

IV. Filter Design

We have to this point avoided putting unnecessary restrictions on the filter coefficients $\{F[k]\}$. In Section II, we have stated

that the elements of $\{F[k]\}$ are real and finite. Section III specified a filter with the further restriction of conjugate-symmetry. However, the conjugate-symmetry condition does not add any restriction to the range of correlation functions which can be simulated, but rather ensures zero cross-correlation between real and imaginary parts at the IDFT output. Hence, the results presented thus far are applicable to any correlation sequence $\{g[d]\}$ which is well approximated in the relation

$$\{g[d]\} \overset{\text{DFT}}{\longleftrightarrow} \left\{(F[k])^2\right\}$$

where $\{(F[k])^2\}$ is a positive real sequence.

A particular set of filter coefficients were provided in the FORTRAN code of [1] without explanation or statistical justification. This specific set of filter coefficients will result in fading statistics modeling the signal received by a vertical monopole antenna under the assumption of isotropic scattering. This model is often used in simulation of multipath fading channels. The theoretical power spectrum of either the real or imaginary (in-phase or quadrature) part of the continuous-time scattered received signal is proportional to [3], [26], [27]

$$S(\phi) = \begin{cases} \dfrac{1}{\pi\phi_m\sqrt{1-(\phi/\phi_m)^2}}, & |\phi| \le \phi_m \\ 0, & \text{elsewhere} \end{cases} \tag{16}$$

where ϕ represents frequency in Hertz and the parameter ϕ_m is the maximum Doppler frequency in Hertz, given by $\phi_m = \nu/\lambda$, where ν is the vehicle velocity in meters/second and λ is the carrier wavelength in meters. The normalized (unit-variance) continuous-time autocorrelation of the scattered received signal under these conditions is $r(\tau) = J_o(2\pi\phi_m\tau)$ [3], [26], [27], where τ is the separation, in seconds, between observation times and $J_0(\cdot)$ is the zeroth-order Bessel function of the first kind.

Ideally, the finite-length sampled sequence (sampling frequency ϕ_s in Hertz) will have the same statistical properties as a sampled version of the theoretical continuous-time signal. That is, we wish the generated sequence to have normalized autocorrelation sequence

$$r[d] = J_0(2\pi f_m |d|) \tag{17}$$

where $f_m = \phi_m/\phi_s$ is the maximum Doppler frequency normalized by the sampling rate and d is the sample lag as previously defined. An exact realization of autocorrelation sequence (17) and the corresponding band-limited power spectrum is not possible with the algorithm. One of the consequences of truncation of the time sequence, inherent in digital simulation since a finite number of channel samples is generated, is *Gibb's oscillations* at discontinuities in the frequency-domain representation of the signal. The effect is that the power spectrum corresponding to the finite-time signal oscillates about that corresponding to the infinite-time signal, and in the case of a band-limited theoretical spectrum, the resulting finite-duration response is no longer band-limited. Furthermore, the resulting frequency response is negative for some frequencies [22], [23]. Since only the magnitude of the filter sequence $\{F[k]\}$ determines the output correlation, the realized power spectrum sequence must be strictly nonnegative, and it is impossible to realize the frequency response of the exact filter.

On the other hand, if we force the power spectrum to be band-limited, we will observe aliasing of the time samples in the finite-length sequence. In practice, however, if the magnitude of the overlapping terms is small, the aliasing error will also be small, but nonetheless a direct implementation of the infinite-time power spectrum cannot yield the exact autocorrelation sequence in this discrete-time system due to time aliasing.

The approach of [1] to defining useful filter coefficients is to sample, in frequency, the continuous-time spectrum (16), at frequencies $k\phi_s/N$, $k = 0, 1, \ldots, N-1$. This effectively ignores finite-time effects. Special treatment is given to the frequency coefficients at two points, though explanation of the choice is given for neither of the two points. The first is the point at zero frequency ($k = 0$), which is made zero. We have explained the benefit of this in the discussion of Section II. The other point, here given the index k_m, is the point at, or just below, the maximum Doppler frequency. That is

$$k_m = \left\lfloor \phi_m \left(\frac{\phi_s}{N}\right)^{-1} \right\rfloor = \lfloor f_m N \rfloor \tag{18}$$

where $\lfloor x \rfloor$ indicates the largest integer less than or equal to x. The coefficient at k_m is chosen in [1] such that the area under an interpolation of the spectrum coefficients is equal to the area under the continuous-time spectrum curve. This is explained as follows (it is not explained in [1]). The realized maximum Doppler frequency in the digital system in Hertz is $k_m\phi_s/N$. The area under the power spectrum curve (16) with the modified Doppler frequency, from zero to analog frequency ϕ, is given by [28, eq. (2.271.4)]

$$C(\phi) \equiv \frac{k_m\phi_s}{N} \arcsin\left(\frac{\phi N}{\phi_s k_m}\right), \qquad 0 \le \phi \le \frac{k_m\phi_s}{N}. \tag{19}$$

The area under the section of the power spectrum between the frequencies represented by samples $(k_m - 1)$ and k_m is equal to $C(k_m\phi_s/N) - C([k_m - 1]\phi_s/N)$. Approximating this area by a rectangle of height $(F[k_m])^2$ and width ϕ_s/N, we obtain

$$F[k_m] = \sqrt{k_m\left[\frac{\pi}{2} - \arctan\left(\frac{k_m - 1}{\sqrt{2k_m - 1}}\right)\right]} \tag{20}$$

the value of $F[k_m]$ used by Smith [1].

The complete filter for use in the modified algorithm of Section III to approximate the correlation function (17) can now be specified as (21), shown at the bottom of the next page.

The filter specification of [1] is clearly not unique. For example, it is also possible to calculate filter coefficients using the relation (9). As has already been noted, this cannot be accomplished exactly since $F[k]$ must be real for all values of d. It is possible, however, to use the relation with $g[d]$ specified by (17) to find the value of $F[k_m]$, and this option has been investigated. Despite the extra computation to obtain $F[k_m]$ in this fashion, it was observed that use of this filter point in the routine resulted in a very small improvement in the quality of the output samples. The measures of Section V were applied to the algorithm with the modified $F[k_m]$. A covariance sequence

length of 200 was considered. The improvement was seen to be roughly 2.5×10^{-4} dB. The filter $\{F_M[k]\}$ gives samples with sufficiently high quality that further improvement is not worthwhile. Statistical averages are observed in practice as time averages, which for a finite number of samples are random variables. Small improvements in autocorrelation accuracy, which are less than the variability in the random time averages, are likely to have negligible effect in any given communication system simulation result. This is the case here.

Also of interest is the effect of having an autocorrelation function with a discontinuous first derivative. If the domain of the IDFT sequence [e.g., in (6) or (A.5)] is extended to include all integers, the resulting sequence is periodic with period N. Since the continuous-time autocorrelation function is symmetric about $\tau = 0$, the discrete-time sequence $\{g[d]\}$ will be symmetric about $d = 0$. The upper half of the sequence $\{g[d]\}$ (that is, $d = N/2, N/2+1, \cdots, N-1$) represents the autocorrelation sequence for negative sample lags. At the point $d = N/2$, the autocorrelation coefficients representing negative sample lags meet the coefficients representing positive sample lags, and the interpolated autocorrelation function may here have a continuous first derivative, or the derivative may be discontinuous. Continuity of the derivative can be ensured by picking f_m such that $J_1(\pi f_m N) = 0$, forcing the derivative of the theoretical autocorrelation to be zero at the crossover point. Imposing this condition usually involves only a very small change in f_m from the design value. Intuitively, we expect that discontinuities will increase high-frequency components in the DFT of the autocorrelation and make the approximation by a band-limited power spectrum less accurate. The quality of the algorithm output with and without the continuous derivative condition was compared using the measures presented in Section V. Length-200 autocorrelation sequences were used in the comparison, with normalized maximum Doppler frequency $f_m = 0.0511$ in the continuous-derivative case, and $f_m = 0.0515$ in the discontinuous-derivative case. The improvement in quality with the continuous derivative autocorrelation was observed to be roughly 1.5×10^{-4} dB for all the measures. With realistic sequence lengths, this is again less than the variability observed in the time autocorrelation from one realization to another, and thus will not be significant in practice.

V. Comparisons

A. The Quantitative Measures

Quantitative quality measures for random variates have been presented in [13]–[15]. The primary purpose of any quality test is to provide a measure of the degree to which the difference between the generated distribution and the ideal distribution affects a typical simulation result. The measures proposed in [13]–[15] directly quantify this difference. The measures represent approximately the difference in signal-to-noise ratio (SNR) predicted to meet a specified performance (error rate, outage, synchronizer jitter, etc.) when an imperfect sequence of random variates is used for simulation rather than a statistically "ideal" sequence.

The measures relate closely to a technique often used to compare performance among communication systems, comparison of the SNR requirement for two systems to achieve the same level of performance with the difference expressed in decibels. For example, it is well known that a 3-dB (or a factor of 2) larger SNR is required in a coherent frequency-shift keying system to achieve equivalent performance to a binary phase-shift keying system. This 3-dB figure is termed the *power margin*. The quality measures described in [13]–[15] use a similar comparison to compare the distribution of variates produced by a random variate generator to a specified Gaussian distribution. The measures are identical to the conventional power margin measure for the univariate case. For the general multivariate case, the exact power margin for a particular event is dependent on the region of integration of the pdf corresponding to the specific event. Provided in [13]–[15] are power margin measures that give an accurate assessment of variate

$$F_M[k] = \begin{cases} 0, & k = 0 \\ \sqrt{\dfrac{1}{2\sqrt{1-\left(\dfrac{k}{Nf_m}\right)^2}}}, & k = 1, 2, \cdots, k_m - 1 \\ \sqrt{\dfrac{k_m}{2}\left[\dfrac{\pi}{2} - \arctan\left(\dfrac{k_m - 1}{\sqrt{2k_m - 1}}\right)\right]}, & k = k_m \\ 0, & k = k_m + 1, \cdots, N - k_m - 1 \\ \sqrt{\dfrac{k_m}{2}\left[\dfrac{\pi}{2} - \arctan\left(\dfrac{k_m - 1}{\sqrt{2k_m - 1}}\right)\right]}, & k = N - k_m \\ \sqrt{\dfrac{1}{2\sqrt{1-\left(\dfrac{N-k}{Nf_m}\right)^2}}}, & k = N - k_m + 1, \cdots, N-2, N-1. \end{cases} \tag{21}$$

quality for an unspecified event region, summarizing the effect of the continuum of power margins in two useful indicators.

The two measures are defined as follows. The first, termed the *mean power margin*, is defined by

$$\mathcal{G}_{\text{mean}} = \frac{1}{\sigma_{\mathbf{X}^2} L} \operatorname{trace}\left\{\mathbf{C}_{\mathbf{X}} \mathbf{C}_{\hat{\mathbf{X}}}^{-1} \mathbf{C}_{\mathbf{X}}\right\} \tag{22}$$

and the second, the *maximum power margin*, is defined by

$$\mathcal{G}_{\max} = \frac{1}{\sigma_{\mathbf{X}^2}} \max\left\{\operatorname{diag}\left\{\mathbf{C}_{\mathbf{X}} \mathbf{C}_{\hat{\mathbf{X}}}^{-1} \mathbf{C}_{\mathbf{X}}\right\}\right\} \tag{23}$$

where $\sigma_{\mathbf{X}}^2$ is the variance of the reference distribution. In (22) and (23), the $L \times L$ matrix $\mathbf{C}_{\hat{\mathbf{X}}}$ is defined to be the covariance matrix of any length-L subset of adjacent variates produced by the random variate generator. Due to the stationarity of the generator output, the covariance matrix of all such subsets will be identical. The $L \times L$ covariance matrix of a reference vector of L ideally distributed variates is similarly defined to be $\mathbf{C}_{\mathbf{X}}$. The matrix $\mathbf{C}_{\mathbf{X}}$ represents the desired covariance matrix, and is known exactly. For some variate generation schemes, the covariance matrix $\mathbf{C}_{\hat{\mathbf{X}}}$ can also be determined exactly. When this is not possible, empirical techniques such as those found in [18, Sec. 13.2] can be used to estimate this matrix.

These measures quantitatively assess the impact of using the approximate pdf of generated samples in a typical simulation application, expressing this impact in a form intuitive to designers of communication systems [13]–[15].

B. Tested Generation Methods

1) IDFT Method: The method used was that of Section III using the filter specified in (21). The Numerical Recipes in C [18] IFFT routine was used for IDFT computation.

2) Filtered WGN: Correlated Rayleigh variates can be generated by filtering two independent zero-mean WGN processes, then adding the two filtered processes in quadrature to form a Rayleigh process. The linear filtering operation on the Gaussian samples yields samples which also have Gaussian distribution. The autocorrelation properties of the resulting sequences are determined by the choice of filter.

Many possibilities for the choice of filter exist. A third-order Butterworth filter is often used [11], [29]. The autocorrelation function of this filter is given by [30]

$$r[\tau] = \sin\left(\frac{\pi}{6}\right) \sum_{l=1}^{3} \exp\left\{-2\pi f_m |\tau| \sin\left(\frac{2l-1}{6}\pi\right)\right\} \cdot \sin\left\{\frac{2l-1}{6}\pi + 2\pi f_m |\tau| \cos\left(\frac{2l-1}{6}\pi\right)\right\}. \tag{24}$$

A different filter specification is given in [14] and [16] which exactly realizes the $J_0(\cdot)$ correlation considered in this paper, as the number of filter taps goes to infinity. This finite impulse response (FIR) filter, of odd length L_f, is given by (25), shown at the bottom of the page.

Quantitative results are provided in this paper both for the autocorrelation given in (24) and for the filter specification given in (25).

3) Sum-of-Sinusoids: A third, popular, method to model the Rayleigh fading channel is to superimpose the outputs from several sinusoidal generators [3], [4]. The ith complex sinusoid is defined by frequency f_{D_i}, phase offset θ_i, and amplitude c_i, where $1 \le i \le N_s$ and N_s is the total number of sinusoids. Thus, the fading process $x[n]$, $n = 0, 1, \cdots, N-1$, is written

$$x[n] = \sum_{i=1}^{N_s} c_i e^{-j(2\pi f_{D_i} n + \theta_i)}. \tag{26}$$

By a central limit theorem [17], as the number of terms becomes large, the sum approaches a complex Gaussian random process. In practice, the generated sequence closely approximates a Gaussian process provided a sufficient number of sinusoids is used. It has been suggested [3], [4] that the Gaussian assumption is closely met for greater than six sinusoids.

The sum-of-sinusoids method implemented here is the Monte Carlo approach given in [4] and [31]. It is shown in [4] that if the frequency of each sinusoid is given by $f_{D_i} = f_m \cos(2\pi u_i)$, where u_i is a random variable uniformly distributed between 0 and 1, and the amplitude of each sinusoid is $1/\sqrt{N_s}$, the fading process approaches that represented by the autocorrelation (17) as $N_s \to \infty$. The random generator is designed to be initialized once at the beginning of the simulation run, then run without further random inputs, as widely implemented [3], [9]. While it is suggested in [4] that for small N_s the generator be reinitialized from time to time in order to improve the channel statistics, no analysis of this method is provided in [4], and the method is not examined here. Sum-of-sinusoids methods are examined in detail in [32]–[36].

C. Comparisons Based on Quality Measures

The four methods of generating correlated random variates given in Section V-B are compared using the quality measures of Section V-A, and these results are presented in Table I. Perfect performance corresponds to 0 dB for all three measures. The reference autocorrelation function for each case is given by (17). An autocorrelation sequence length of 200 was considered, at a normalized maximum Doppler of $f_m = 0.05$. In the case of the IDFT method and FIR filtering using (25), both a theoretical autocorrelation function and an empirically

$$h[n] = \begin{cases} (f_m)^{1/2} \dfrac{\Gamma(3/4)}{\Gamma(5/4)}, & n = \dfrac{L_f - 1}{2} \\ \left(\dfrac{f_m}{\pi}\right)^{1/4} \Gamma\left(\dfrac{3}{4}\right) \left[n - \dfrac{L_f-1}{2}\right]^{-1/4} J_{1/4}\left(2\pi f_m \left[n - \dfrac{L_f-1}{2}\right]\right), & n = 0, 1, \cdots, L_f - 1;\ n \ne \dfrac{L_f-1}{2} \end{cases} \tag{25}$$

TABLE I
A COMPARISON OF FOUR METHODS OF GENERATING CORRELATED RAYLEIGH VARIATES FOR COVARIANCE SEQUENCE LENGTH 200, USING THEORETICALLY DETERMINED (T) AND EMPIRICALLY DETERMINED (E) AUTOCORRELATION FUNCTIONS

		$\mathcal{G}_{\text{mean}}$	$\mathcal{G}_{\text{max}}$
IDFT Method	(T)	0.00076 dB	0.00081 dB
	(E)	0.0034 dB	0.0038 dB
FIR Filtering	length-31 (T)	2.4 dB	2.6 dB
	length-31 (E)	2.4 dB	2.5 dB
	length-127 (T)	0.87 dB	0.95 dB
	length-127 (E)	0.86 dB	0.93 dB
	length-1023 (T)	0.084 dB	0.092 dB
	length-1023 (E)	0.086 dB	0.093 dB
	length-4095 (T)	0.020 dB	0.021 dB
	length-4095 (E)	0.019 dB	0.020 dB
Sum of Sinusoids	16 sinusoids (E)	17.9 dB	21.5 dB
	64 sinusoids (E)	2.2 dB	2.6 dB
	256 sinusoids (E)	0.25 dB	0.29 dB
3rd order Butterworth Approximation		2.7 dB	2.9 dB

determined autocorrelation function were tested. The theoretical functions were obtained using (9) and (25), respectively. In the case of the third-order Butterworth approximation, the autocorrelation function given in (24) was used. Empirical autocorrelation functions were used in evaluation of the quality measures for the sum-of-sinusoids method owing to stability problems with the theoretical expressions. Where used, empirical correlations were found using the method of [18, p. 546] on 2^{20} generated samples.

In this comparison, the IDFT method stands out as being clearly superior to the competing methods, closely matching the reference pdf over the 200-sample interval. Good quality can be achieved with filtering using (25) and the sum-of-sinusoids method, but long FIR filter lengths and large numbers of sinusoids were observed to be necessary for these correlation properties to be obtained. The third-order Butterworth approximation was observed to be poor over the 200-sample interval, with slightly worse quality than the length-31 FIR filter.

D. Comparisons Based on Execution Time

In order to assess the relative computational effort to generate samples using different methods, two sets of tests were performed. The first test compared computation times for generation of sequences of length $2^{21} = 2\,097\,152$ on an UltraSPARC machine using routines coded in C. The normalized maximum Doppler frequency was $f_m = 0.05$ in each case. The FIR filtering method was implemented both by directly computing the convolution sum and using FFT operations. For the sum-of-sinusoids method, lookup tables were not used; use of lookup tables for computation of the sinusoids would reduce the required computational effort per sample.

Results for the time comparisons are presented in Fig. 4. The IDFT method of Section V-B.1 is clearly superior in this regard. The direct FIR filtering method can be performed quickly only for very short filter lengths, and is observed to be very inefficient for long filter lengths. Performing FIR filtering using the FFT is seen to be much more efficient than the direct FIR method at long filter lengths, but still roughly three times more time is needed to generate the samples in comparison to the IDFT approach. The sum-of-sinusoids approach was also seen to require much more effort than the IDFT method, for even a small number of sinusoids. The comparison was similar for the case of generating 2^{16} samples.

The second set of tests compared the number of floating-point operations per sample to obtain output sequences using each routine coded in MATLAB, as a function of sequence length. In all tests using the IDFT, the number of points was restricted to a power of two. Even with this restriction, the number of floating-point operations per sample is not constant with the IDFT method, due to the $O(N \log N)$ time complexity of the FFT operation. However, it will be observed that the inherent efficiency of the FFT outweighs the effect of the $\log N$ factor for practical sequence lengths.

Direct FIR filtering was performed using the MATLAB function `filter`. Fig. 5 shows the floating-point operations per sample using this direct FIR filtering routine together with the floating-point operations per sample using the IDFT routine. It is observed that the IDFT uses much fewer floating-point operations to generate the samples than even relatively short FIR filters producing inferior correlation properties. The number of operations per sample to perform the direct FIR filtering method is constant, with additional operations required to generate the filter coefficients which increase the overall operations per sample for short output sequences.

Fig. 6 shows the number of floating-point operations per sample for the FIR method using the overlap-add approach implemented in the MATLAB function `fftfilt.m`. These results are plotted with those for the IDFT method, and once again the IDFT method is observed to use fewer floating-point operations per sample. The number of operations per sample is nearly constant for large N, due to the fixed FFT length in this method, but once again the increase in operations per sample with N for the IDFT method is seen to have minimal effect on the comparison for practical sequence lengths.

Finally, Fig. 7 plots the comparison for the sum-of-sinusoids method. The number of floating-point operations per sample for the sum-of-sinusoids method is essentially constant, since initialization of this routine is not computationally significant. The IDFT method is again observed to require fewer operations, even for small N_s.

VI. CONCLUSIONS

A new IDFT method for the generation of correlated Rayleigh and Ricean random variates has been presented. Analysis of the

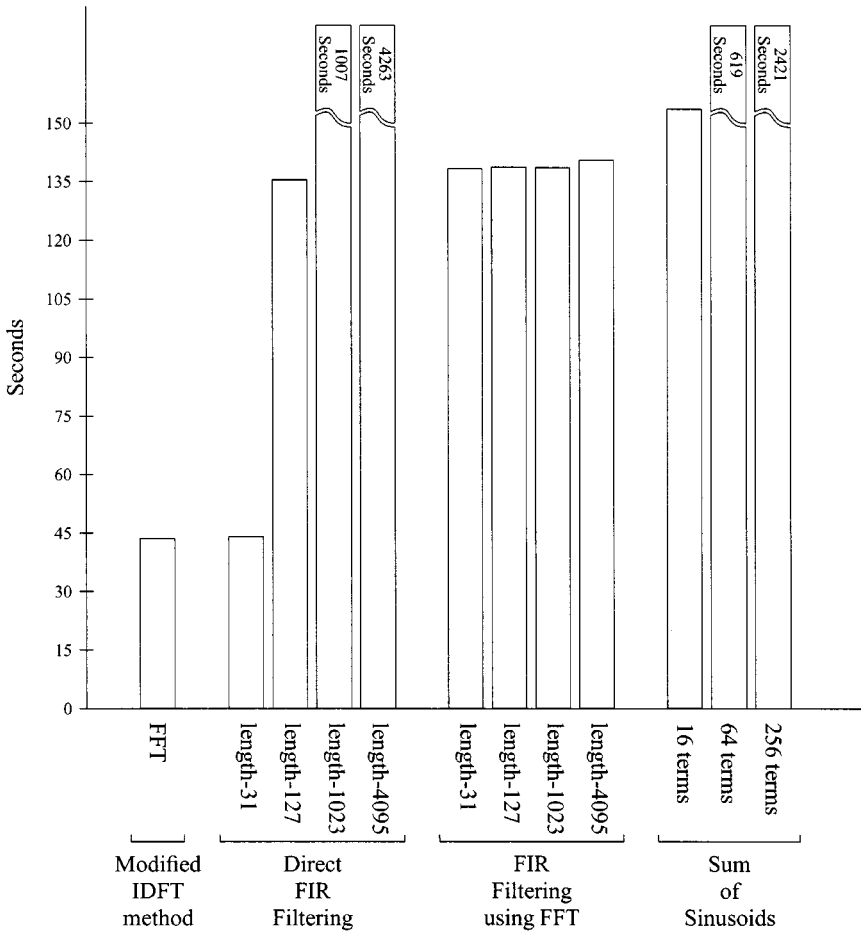

Fig. 4. The time to generate 2^{21} complex samples using different generation methods.

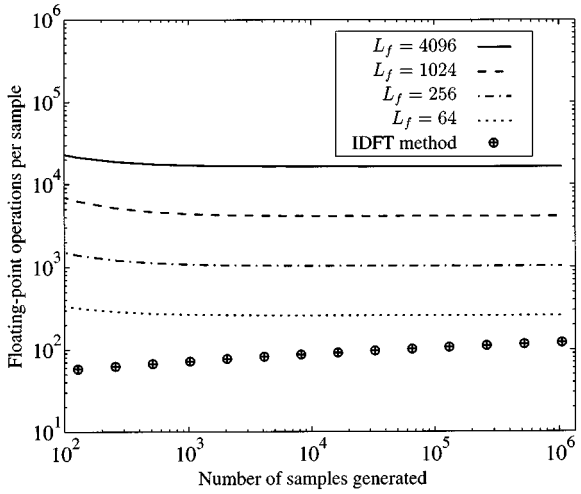

Fig. 5. Number of floating-point operations to generate samples using the direct FIR filtering method, plotted with the number of floating-point operations to generate samples using the IDFT method, as a function of the number of samples generated. The number of points in the IDFT method is a power of two.

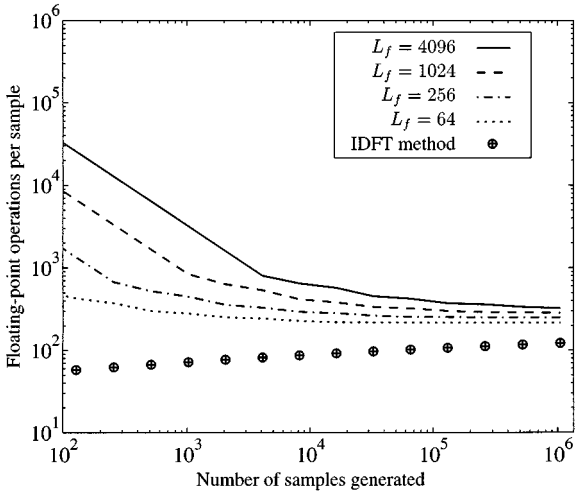

Fig. 6. Number of floating-point operations to generate samples using overlap-add FIR filtering method via `fftfilt.m`, plotted with the number of floating-point operations to generate samples using the IDFT method, as a function of the number of samples generated. The number of points in the IDFT method is a power of two.

statistical properties of this method and the original method of Smith [1] has been provided, along with a discussion of filter coefficients applicable to a common fading model. A quantitative comparison of the IDFT method with three other algorithms has also been presented. Considering both computational effort and the quality of the generated samples, the IDFT method of Section III clearly stands out as being superior to the other tested methods. Accurate correlation between the generated samples

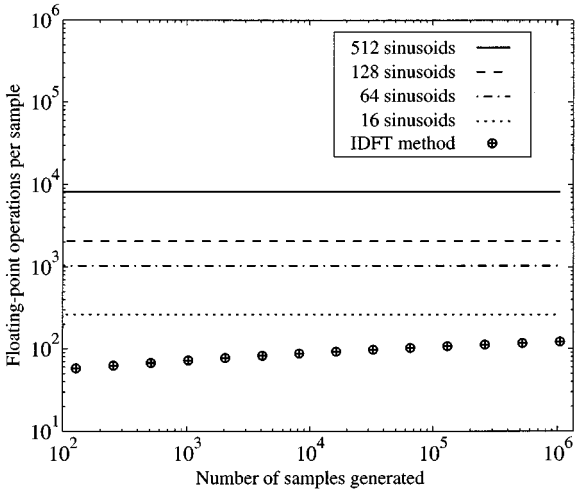

Fig. 7. Number of floating-point operations to generate samples using the sum-of-sinusoids method, plotted with the number of floating-point operations to generate samples using the IDFT method, as a function of the number of samples generated. The number of points in the IDFT method is a power of two.

is produced over a wide range of sample lags, and the time requirement to generate the samples is less than the other methods considered.

One advantage of both the direct FIR filtering method and the sum-of-sinusoids method is that samples can be generated as they are needed. In contrast, the IDFT method requires that all samples be generated using a single fast Fourier transform operation. Clearly, however, the reduced storage requirements of the former two methods come at the expense of overall computational effort and/or variate quality. The memory available on modern workstations and personal computers allows quick generation of a large number of high-quality samples using the IDFT method. Also, interpolation can be used in many practical cases (see [12] and [37]) to reduce the required number of generated channel samples and hence the IDFT size. In summary, the comparisons show the IDFT method to be the most efficient and highest quality method among the tested approaches to correlated Rayleigh variate generation.

Appendix A
Mean and Autocorrelation of the IDFT Output Sequences

We can write

$$x_R[n] = \frac{1}{N}\sum_{k=0}^{N-1} F[k]A[k]\cos\frac{2\pi kn}{N} + \frac{1}{N}\sum_{k=0}^{N-1} F[k]B[k]\sin\frac{2\pi kn}{N} \quad \text{(A.1)}$$

and

$$x_I[n] = \frac{1}{N}\sum_{k=0}^{N-1} F[k]A[k]\sin\frac{2\pi kn}{N} - \frac{1}{N}\sum_{k=0}^{N-1} F[k]B[k]\cos\frac{2\pi kn}{N}. \quad \text{(A.2)}$$

Taking the ensemble average of the real part $\{x_R[n]\}$, we observe

$$\begin{aligned} E\{x_R[n]\} &= \frac{1}{N}\sum_{k=0}^{N-1}\left[E\{A[k]\}F[k]\cos\left(\frac{2\pi kn}{N}\right) + E\{B[k]\}F[k]\sin\left(\frac{2\pi kn}{N}\right)\right] \\ &= 0 \end{aligned}$$

since $E\{A[k]\}$ and $E\{B[k]\}$ are both zero from (1). The ensemble average of the imaginary part $\{x_I[n]\}$ is also zero, which can be shown similarly.

Considering next the autocorrelation of the real part, we write this quantity as the equation shown at the bottom of the page. Expanding this product, and making use of the fact that the

$$\begin{aligned} r_{RR}[m,n] &= E\{x_R[m]x_R[n]\} \\ &= E\left\{\left[\underbrace{\frac{1}{N}\sum_{k=0}^{N-1} F[k]A[k]\cos\frac{2\pi km}{N} + \frac{1}{N}\sum_{k=0}^{N-1} F[k]B[k]\sin\frac{2\pi km}{N}}_{2N\text{ terms}}\right]\right. \\ &\quad \left.\cdot\left[\underbrace{\frac{1}{N}\sum_{l=0}^{N-1} F[l]A[l]\cos\frac{2\pi ln}{N} + \frac{1}{N}\sum_{l=0}^{N-1} F[l]B[l]\sin\frac{2\pi ln}{N}}_{2N\text{ terms}}\right]\right\}. \end{aligned}$$

expectation operator is linear, we obtain

$$\begin{aligned} r_{RR}[m,n] = E\left\{\left[\frac{1}{N}\sum_{k=0}^{N-1} F[k]A[k]\cos\left(\frac{2\pi km}{N}\right)\right]\right. \\ \left.\cdot\left[\frac{1}{N}\sum_{k=0}^{N-1} F[k]A[k]\cos\left(\frac{2\pi kn}{N}\right)\right]\right\} \\ + E\left\{\left[\frac{1}{N}\sum_{k=0}^{N-1} F[k]A[k]\cos\left(\frac{2\pi km}{N}\right)\right]\right. \\ \left.\cdot\left[\frac{1}{N}\sum_{k=0}^{N-1} F[k]B[k]\sin\left(\frac{2\pi kn}{N}\right)\right]\right\} \\ + E\left\{\left[\frac{1}{N}\sum_{k=0}^{N-1} F[k]B[k]\sin\left(\frac{2\pi km}{N}\right)\right]\right. \\ \left.\cdot\left[\frac{1}{N}\sum_{k=0}^{N-1} F[k]A[k]\cos\left(\frac{2\pi kn}{N}\right)\right]\right\} \\ + E\left\{\left[\frac{1}{N}\sum_{k=0}^{N-1} F[k]B[k]\sin\left(\frac{2\pi km}{N}\right)\right]\right. \\ \left.\cdot\left[\frac{1}{N}\sum_{k=0}^{N-1} F[k]B[k]\sin\left(\frac{2\pi kn}{N}\right)\right]\right\}. \end{aligned} \tag{A.3}$$

The first of the four terms can be expressed as

$$\frac{\sigma^2}{N^2}\sum_{k=0}^{N-1}(F[k])^2\cos\left(\frac{2\pi km}{N}\right)\cos\left(\frac{2\pi kn}{N}\right)$$

using (3). The last of the four terms in (A.3) is simplified similarly, yielding

$$\frac{\sigma^2}{N^2}\sum_{k=0}^{N-1}(F[k])^2\sin\left(\frac{2\pi km}{N}\right)\sin\left(\frac{2\pi kn}{N}\right).$$

Both of the middle terms in (A.3) are zero from (4).

Now, using well-known trigonometric identities [38, eqs. (5.65), (5.66)], we can rewrite $r_{RR}[m,n]$ as

$$\begin{aligned} r_{RR}[m,n] &= \frac{\sigma^2}{N^2}\sum_{k=0}^{N-1}(F[k])^2\cos\frac{2\pi k(m-n)}{N} \\ &= \frac{\sigma^2}{N^2}\sum_{k=0}^{N-1}(F[k])^2\cos\frac{2\pi kd}{N} = r_{RR}[d] \end{aligned} \tag{A.4}$$

where the *sample lag* d is defined to be the distance between samples

$$d \equiv (n-m).$$

The autocorrelation of the sequence $\{x_I[n]\}$ can be shown, using the same technique, to be identical to $r_{RR}[d]$.

Considering a general real-valued $\{F[k]\}$, we write

$$\begin{aligned} r_{RR}[d] &= r_{II}[d] \\ &= \frac{\sigma^2}{2N^2}\sum_{k=0}^{N-1}(F[k])^2 e^{j(2\pi kd/N)} \\ &\quad + \frac{\sigma^2}{2N^2}\sum_{k=0}^{N-1}(F[k])^2 e^{-j(2\pi kd/N)} \\ &= \frac{\sigma^2}{2N}\left[\left\{\frac{1}{N}\sum_{k=0}^{N-1}(F[k])^2 e^{j(2\pi kd/N)}\right\}\right. \\ &\quad \left. + \left\{\frac{1}{N}\sum_{k=0}^{N-1}(F[k])^2 e^{j(2\pi kd/N)}\right\}^*\right] \end{aligned}$$

where * denotes complex conjugation. Let the sequence $\{(F[k])^2\}$ have IDFT

$$g[d] = \frac{1}{N}\sum_{k=0}^{N-1}(F[k])^2 e^{j(2\pi kd/N)}. \tag{A.5}$$

Then

$$r_{RR}[d] = r_{II}[d] = \frac{\sigma^2}{2N}\left(g[d] + g^*[d]\right) = \frac{\sigma^2}{N}\,\mathrm{Re}\{g[d]\}. \tag{A.6}$$

So, the autocorrelations of $\{x_R[n]\}$ and $\{x_I[n]\}$ are dependent only on the real part of $\{g[d]\}$, and $\{F[k]\}$ and $\{g[d]\}$ are related by

$$\{g[d]\} \overset{\mathrm{DFT}}{\longleftrightarrow} \{(F[k])^2\}. \tag{A.7}$$

The cross-correlation between the real and imaginary parts of the IDFT output sequence can be derived similarly. This cross-correlation $r_{RI}[d]$ is given by

$$r_{RI}[d] = \frac{\sigma^2}{N}\,\mathrm{Im}\{g[d]\}. \tag{A.8}$$

Appendix B
Ergodicity of the Algorithm Output

The property of equality between an ensemble average and an infinite-time average is referred to as an *ergodic property* [39]. We will now show that the complex Gaussian process at the output of the IDFT has this property for both mean and autocorrelation.

The time average of the random process $\{x[n]\}$ is

$$\langle x[n]\rangle = \frac{1}{N}\sum_{n=0}^{N-1} x[n] = \frac{1}{N}F[0]\left(A[0] - jB[0]\right). \tag{B.1}$$

The time average $\langle x[n]\rangle$ is a random variable with mean

$$E\{\langle x[n]\rangle\} = E\left\{\frac{1}{N}\sum_{n=0}^{N-1} x[n]\right\} = E\{x[n]\} \tag{B.2}$$

which has been shown to be zero, and variance

$$\begin{aligned} &E\{\langle x[n]\rangle \langle x[n]\rangle^*\} - E\{\langle x[n]\rangle\} E\{\langle x[n]\rangle\}^* \\ &\quad = E\left\{\frac{1}{N}(F[0]A[0] - jF[0]B[0]) \right. \\ &\qquad \left. \cdot \frac{1}{N}(F[0]A[0] + jF[0]B[0])\right\} - 0 \\ &\quad = \frac{1}{N^2}(F[0])^2\left[E\left\{(A[0])^2\right\} + E\left\{(B[0])^2\right\}\right] \\ &\quad = \frac{2\sigma^2}{N^2}(F[0])^2. \end{aligned}$$

The quantity $(\sigma F[0])^2$ is finite and constant; therefore

$$\frac{2\sigma^2}{N^2}(F[0])^2 \to 0 \quad \text{as} \quad N \to \infty. \tag{B.3}$$

The mean ergodicity of $\{x[n]\}$ is implied by (B.2) and (B.3).

From the discussion of [39, Sec. 8.2, 8.4], a zero-mean stationary Gaussian process X is said to possess mean-square ergodicity of the autocorrelation if and only if

$$\lim_{T\to\infty}\frac{1}{2T}\int_{-T}^{T} C_X^2(u)\,du = 0$$

where $C_X(\tau)$ is the continuous autocovariance function for process X. The autocovariance is an even function, and therefore we may also write the condition as

$$\lim_{T\to\infty}\frac{1}{T}\int_{0}^{T} C_X^2(u)\,du = 0. \tag{B.4}$$

We do not know the autocovariance function for all time—we have only samples of the function over a finite interval. However, we can approximate the integral by a Riemann sum [40], with the function evaluated only at the sample points of our discrete-time system.

Partitioning the interval $[0,T]$ into N subintervals of equal width $\Delta = (T/N)$, the definite integral from 0 to T is given by the limit of the Riemann sum

$$\int_0^T C_X^2(u)\,du = \lim_{\Delta\to 0}\sum_{d=0}^{N-1}(C_X(d\Delta))^2\Delta.$$

The partition width Δ, which corresponds to the sampling period of the discrete-time system, should be such that the approximation to the integral given by the sum is very good. This will be true since the sampling rate is usually much greater than twice the maximum Doppler frequency, and thus the baseband fading signal is densely sampled. The function $C_X(dT/N)$ represents samples of the autocorrelation function for the IDFT output, where T is the sequence length and N is the number of samples. Assuming that the integral is well approximated, and substituting the sum for the integral in (B.4), we obtain the approximate expression

$$\begin{aligned} \lim_{T\to\infty}\frac{1}{T}\int_0^T C_X^2(u)\,du &\approx \lim_{T\to\infty}\frac{1}{T}\left\{\frac{T}{N}\sum_{d=0}^{N-1}\left[C_X\left(d\,\frac{T}{N}\right)\right]^2\right\} \\ &= \lim_{T\to\infty}\frac{1}{N}\sum_{d=0}^{N-1}\left[\frac{\sigma^2}{N}\operatorname{Re}\{g[d]\}\right]^2. \end{aligned}$$

Writing $\{g[d]\}$ as the inverse DFT of $\{(F[k])^2\}$, the expression becomes

$$\begin{aligned} &\lim_{T\to\infty}\frac{1}{N}\sum_{d=0}^{N-1}\left[\frac{\sigma^2}{N}\operatorname{Re}\left\{\frac{1}{N}\sum_{k=0}^{N-1}(F[k])^2 e^{(j2\pi kd/N)}\right\}\right]^2 \\ &\quad = \lim_{T\to\infty}\frac{\sigma^4}{N^5}\sum_{d=0}^{N-1}\left[\sum_{k=0}^{N-1}\operatorname{Re}\left\{(F[k])^2 e^{(j2\pi kd/N)}\right\}\right]^2. \end{aligned}$$

Now, for a fixed sampling rate in the discrete-time system, N will approach infinity as T does. Since

$$\begin{aligned} &\lim_{T\to\infty}\frac{\sigma^4}{N^5}\sum_{d=0}^{N-1}\left(\sum_{k=0}^{N-1}\operatorname{Re}\left\{(F[k])^2 e^{-(j2\pi kd/N)}\right\}\right)^2 \\ &\quad \le \lim_{N\to\infty}\frac{\sigma^4}{N^5}\sum_{d=0}^{N-1}\left(N\max_k\left\{\left|(F[k])^2\right|\right\}\right)^2 \\ &\quad = \lim_{N\to\infty}\frac{\sigma^4}{N^2}\max_k (F[k])^4 \end{aligned} \tag{B.5}$$

and the power spectrum $\{(F[k])^2\}$ is finite for all k in the digital system, clearly, the limit is zero and we can say

$$\lim_{T\to\infty}\frac{1}{T}\left\{\frac{T}{N}\sum_{d=0}^{N-1}\left[C_X\left(d\,\frac{T}{N}\right)\right]^2\right\} = 0.$$

Thus, we have shown the output of the random generator to be autocorrelation ergodic, under the assumption that the sampling rate of this system is such that the autocorrelation function is densely sampled (or equivalently, that f_m is small). The limit condition in (B.5) is not tight, so we would expect this condition to hold for any practical case.

Since the Gaussian process is fully specified by the mean and autocorrelation function, it follows that the complex Gaussian output of the simulator is ergodic.

REFERENCES

[1] J. I. Smith, "A computer generated multipath fading simulation for mobile radio," *IEEE Trans. Veh. Technol.*, vol. VT-24, pp. 39–40, Aug. 1975.

[2] D. J. Young and N. C. Beaulieu, "On the generation of correlated Rayleigh random variates by inverse discrete Fourier transform," in *1996 5th IEEE Int. Conf. on Universal Personal Communications Rec.*, Cambridge, MA, Sept. 1996, pp. 231–235.

[3] W. Jakes, *Microwave Mobile Communications*. New York: Wiley, 1974.
[4] P. Hoeher, "A statistical discrete-time model for the WSSUS multipath channel," *IEEE Trans. Veh. Technol.*, vol. 41, pp. 461–468, Nov. 1992.
[5] M. Pätzold, U. Killat, and F. Laue, "A deterministic digital simulation model for Suzuki processes with application to a shadowed Rayleigh land mobile radio channel," *IEEE Trans. Veh. Technol.*, vol. 45, pp. 318–331, May 1996.
[6] G. Benelli, "A Go-Back-N protocol for mobile communications," *IEEE Trans. Veh. Technol.*, vol. 40, pp. 714–720, Nov. 1991.
[7] H. B. Li, Y. Iwanami, and T. Ikeda, "Symbol error rate analysis for MPSK under Rician fading channels with fading compensation based on time correlation," *IEEE Trans. Veh. Technol.*, vol. 44, pp. 535–541, Aug. 1995.
[8] P. Dent, G. E. Bottomley, and T. Croft, "Jakes fading model revisited," *Electron. Lett.*, vol. 29, no. 3, pp. 1162–1163, June 24 1993.
[9] G. Stüber, *Principles of Mobile Communication*. Boston, MA: Kluwer, 1996.
[10] H.-Y. Wu and A. Duel-Hallen, "On the performance of coherent and noncoherent multiuser detectors for mobile radio CDMA channels," in *1996 5th IEEE Int. Conf. on Universal Personal Commun. Rec.*, Cambridge, MA, Sept. 1996, pp. 76–80.
[11] C. Loo and N. Secord, "Computer models for fading channels with applications to digital transmission," *IEEE Trans. Veh. Technol.*, vol. 40, pp. 700–707, Nov. 1991.
[12] P. M. Crespo and J. Jiménez, "Computer simulation of radio channels using a harmonic decomposition technique," *IEEE Trans. Veh. Technol.*, vol. 44, pp. 414–419, Aug. 1995.
[13] D. J. Young and N. C. Beaulieu, "Quality measures for random variate generation," in *1998 Int. Conf. on Commun. (ICC'98) Rec.*, Atlanta, GA, June 1998, pp. 1451–1455.
[14] D. J. Young, "The generation of correlated Rayleigh random variates by discrete Fourier transform and quality measures for random variate generation," M.S. thesis, Queen's Univ., Kingston, ON, Canada, 1997.
[15] D. J. Young and N. C. Beaulieu, "Quality measures for random variates," IEEE Trans. Inform. Theory, submitted for publication.
[16] D. Verdin and T. Tozer, "Generating a fading process for the simulation of land-mobile radio communications," *Electron. Lett.*, vol. 29, no. 23, pp. 2011–2012, Nov. 11 1993.
[17] A. Papoulis, *Probability, Random Variable, and Stochastic Processes*, 3rd ed. New York: McGraw-Hill, 1991.
[18] W. Press *et al.*, *Numerical Recipes in C, The Art of Scientific Computing*. Cambridge, U.K.: Cambridge Univ. Press, 1992.
[19] L. DeVroye, *Non-Uniform Random Variate Generation*. New York: Springer-Verlag, 1986.
[20] IEEE ASSP Group DSP Committee, *Programs for Digital Signal Processing*. New York: IEEE Press, 1979.
[21] J. G. Proakis, *Digital Communications*, 2nd ed. New York: McGraw-Hill, 1989.
[22] J. G. Proakis and D. G. Manolakis, *Digital Signal Processing: Principles, Algorithms, and Applications*. Upper Saddle River, NJ: Prentice-Hall, 1996.
[23] A. V. Oppenheim and R. W. Schafer, *Discrete-Time Signal Processing*. Englewood Cliffs, NJ: Prentice-Hall, 1989.
[24] IMSL, Inc., *FORTRAN Subroutines for Mathematical Applications* Houston, TX, 1991.
[25] N. C. Beaulieu and C. C. Tan, "FFT based generation of bandlimited gGaussian noise variates," *Eur. Trans. Telecommun.*, vol. 10, pp. 545–550, Sept./Oct. 1999.
[26] R. H. Clarke, "A statistical theory of mobile-radio reception," *Bell Syst. Tech. J.*, vol. 47, pp. 957–1000, July/Aug. 1968.
[27] M. J. Gans, "A power-spectral theory of propagation in the mobile-radio environment," *IEEE Trans. Veh. Technol.*, vol. VT-21, pp. 27–38, Feb. 1972.
[28] I. S. Gradshteyn, I. M. Ryzhik, and A. Jeffrey, *Table of Integrals, Series, and Products*, 5th ed. San Diego, CA: Academic, 1994.
[29] P. McLane, "Two-stage doppler-phasor-corrected TCM/DMPSK for shadowed mobile satellite channels," *IEEE Trans. Commun.*, vol. 41, pp. 1137–1141, Aug. 1993.
[30] N. C. Beaulieu, "On the performance of digital detectors with dependent samples," *IEEE Trans. Commun.*, vol. 36, pp. 1248–1253, Nov. 1988.
[31] H. Schulze, "Stochastic models and digital simulation of mobile channels" (in German), in *Proc. Kleinheubacher Berichte*, vol. 32. Darmstadt, 1989.
[32] M. F. Pop and N. C. Beaulieu, "Statistical investigation of sum-of-sinusoids fading channel simulators," in *GLOBECOM'99 Conf. Rec.*, Rio de Janeiro, Brazil, Dec. 1999, pp. 419–426.
[33] ——, "Limitations of sum-of-sinusoids fading channel simulators," IEEE Trans. Commun., to be published.
[34] M. F. Pop, "Statistical analysis of sum-of-sinusoids fading channel simulators," M.Sc. thesis, Queen's Univ., Kingston, ON, Canada, 1999.
[35] M. Pätzold, U. Killat, F. Laue, and Y. Li, "On the statistical properties of deterministic simulation models for mobile fading channels," *IEEE Trans. Veh. Technol.*, vol. 47, pp. 254–269, Feb. 1998.
[36] M. Pätzold and F. Laue, "Statistical properties of Jakes fading channel simulator," in *VTC'98 Conf. Rec.*, Ottawa, ON, Canada, May 1998, pp. 712–718.
[37] S. A. Fechtel, "A novel approach to modeling and efficient simulation of frequency-selective fading radio channels," *IEEE J. Select. Areas Commun.*, vol. 11, pp. 422–431, Apr. 1993.
[38] M. R. Spiegel, *Mathematical Handbook of Formulas and Tables*. New York: McGraw-Hill, 1968.
[39] W. A. Gardner, *Introduction to Random Processes*. New York: Macmillan, 1986.
[40] W. Rudin, *Principles of Mathematical Analysis*. New York: McGraw-Hill, 1964.

David J. Young (S'92) was born in Hamilton, ON, Canada, in 1971. He received the B.Sc.(Eng) and M.Sc.(Eng) degrees in 1994 and 1997, respectively, both from Queen's University, Kingston, ON, Canada. He is currently working toward the Ph.D. degree in the Department of Electrical and Computer Engineering at Queen's University. He is the receipient of an Ontario Graduate Scholarship in Science and Technology, an R.S. McLaughlin Graduate Fellowship (declined), and three Queen's Graduate Awards.

His research interests include fading channel simulation and multitone transmission systems.

Norman C. Beaulieu (S'82–M'86–SM'89–F'99) received the B.A.Sc. (honors), M.A.Sc., and Ph.D. degrees in electrical engineering in 1980, 1983, and 1986, respectively, from the University of British Columbia, Vancouver, BC, Canada. In 1980, he was awarded the University of British Columbia Special University Prize in Applied Science.

He held an appointment as Queen's National Scholar Assistant Professor in the Department of Electrical Engineering at Queen's University, Kingston, ON, Canada, from September 1986 to June 1988. During the time July 1988 to June 1993, he held the position of Associate Professor. Since July 1993, he has been a Professor of Electrical Engineering at Queen's. His current research interests include digital communications over fading channels, interference effects in digital modulations, channel modeling and simulation, decision-feedback equalization, and digital synchronization in sampled receivers.

Dr. Beaulieu is a member of the Communication Theory Committee. He served as representative of the Communication Theory Committee to the Technical Program Committee of the 1991 International Conference on Communications and as co-representative of the Communication Theory Committee to the Technical Program Committee of the 1993 International Conference on Communications and the 1996 International Conference on Communications. He was General Chair of the Sixth Communication Theory Mini-Conference in association with GLOBECOM'97. Presently, he is serving as Co-Chair of the Canadian Workshop on Information Theory 1999. Since January 1992, he has served as Editor for Wireless Communication Theory of the IEEE TRANSACTIONS ON COMMUNICATIONS. Since November 1996, he has served as Associate Editor for Wireless Communication Theory of the IEEE COMMUNICATIONS LETTERS. Effective January 2000, Dr. Beaulieu was appointed Editor-in-Chief of the IEEE TRANSACTIONS ON COMMUNICATIONS. He was a recipient of the Natural Science and Engineering Research Council (NSERC) E.W.R. Steacie Memorial Fellowship in 1999.